IONIZATION-INDUCED TRAPPING IN LASER-PLASMA ACCELERATORS AND SYNCHROTRON RADIATION FROM THE BETATRON OSCILLATION*

M. Chen†, E. Esarey, C.G.R. Geddes, C.B. Schroeder, W.P. Leemans,
LOASIS Program, LBNL, Berkeley, CA 94720, USA
E. Cormier-Michel, D.L. Bruhwiler, Tech-X Corporation, Boulder, CO 80303, USA

Abstract

Ionization injection into a laser wakefield accelerator is studied by multi-dimensional particle-in-cell (PIC) simulations. To obtain low energy spread beams we use a short region of gas mixture (H+N) near the start of the stage to trap electrons, while the remainder of the stage uses pure H and is injection-free. Effects of gas mix parameters, including concentration and length of the mixture region, on the final electron injection number and beam quality are studied. Two dimensional PIC simulations show the injected electron beam has filament structures in the plane perpendicular to the laser polarization direction in early time and this structure disappears later due to the betatron oscillation of the electrons in the wakefield. Synchrotron radiation from the accelerated electrons is calculated by a post processing code - Virtual Detector for Synchrotron Radiation (VDSR).

INTRODUCTION

Laser-plasma accelerators are of great interest because of their ability to sustain extremely large acceleration gradients, enabling a compact accelerating structure [1]. Recently GeV mono-energetic electron beams have been demonstrated in experiments within centimetre scale [2, 3]. To better use these accelerated beams, such as in an undulator for radiation sources, beam quality still needs to be improved, especially the energy spread [4, 5, 6] and transverse emittance. To get high quality beams, in addition to the acceleration process, the beam injection and trapping should also be well controlled [7, 8]. Electron injection in the laser wakefield has obtained great progress recently in experiments by using plasma density control [9, 10], or trigged by multiple colliding laser pulses [8], or by ionizing high order electrons of the background ions [11, 12, 13]. To further improve the beam quality, in this paper, we study the last scheme in detail to understand the relationship between the experimental conditions and the final beam quality. Finally we also calculated the accelerated beam's betatron radiation in the wakefield by a post processing code (VDSR).

* Work supported by the U.S. Department of Energy under Contract No. DE-AC02-05CH11231, the National Science Foundation, National Nuclear Security Administration, NA-22, and by Tech-X Corporation. NERSC computational resources were used.

† Minchen@lbl.gov

IONIZATION INJECTION

Electrons to be trapped should have an initial energy which is larger than a threshold which depends on the phase position of the electrons in the wake. Typically the wakefield has a phase velocity closed to the laser group velocity $v_g = (1 - \omega_p^2/\omega_0^2)c$, where c is the light speed in vacuum, ω_p and ω_0 are the plasma and laser frequency, respectively. In the ionization injection scheme, electrons of the inner shell are ionized near the peak of the laser pulse, which makes their trapping threshold much lower than the pre-ionized back ground electrons which usually have negative longitudinal momenta at this phase. From one dimensional wakefield theory we know the trapping condition for ionized electrons is [14]:

$$H_i = 1 - \phi(\xi_i) \leq H_s = \gamma_\perp \gamma_p^{-1} - \phi_{\min}, \qquad (1)$$

where ξ_i is the ionization phase position of the electrons in the wakefield, γ_p is the relativistic factor of the wake, $\phi_{\min}$ is the minimum potential of the wakefield, $\gamma_\perp = \sqrt{1+p_\perp^2} = \sqrt{1+a_\perp^2(\xi_i)}$ and $a_\perp = eA/m_e c^2$ is the normalized vector potential of the laser pulse. As we see if $\phi(\xi_i)$ is large enough, the electrons born at ξ_i can be trapped by the wakefield. Ionization trapping can happen by using two crossing pulses [15] or by a single pulse going through a neutral gas medium [11]. For a single pulse scheme, to reduce the beam energy spread, electron injection should happen within a short region, otherwise energy spread will increase due to the different acceleration lengths of the trapped electrons. Additionally, as we will see, continuously electron injection makes beam load effects severe, which reduces the final injection number.

Gas Length and Concentration Effects

To study the effect of the gas conditions on the final electron beam we did particle-in-cell simulations by use of the ionization included in the VLPL code [16]. To save computational time we use electrons (instead of Hydrogen atoms) and Nitrogen atoms as the background plasma. The normalized electron density $n_e = 0.001\ n_c$ (initial free electron density plus Nitrogen density times 5) is made uniform throughout the plasma after a ramp region (20 λ_0 long) in the beginning of the plasma to avoid boundary injection, where $n_c = 1.7 \times 10^{21}/cm^3$ is the critical density for a laser of $800nm$ wavelength ($\lambda_0 = 800\ nm$). We

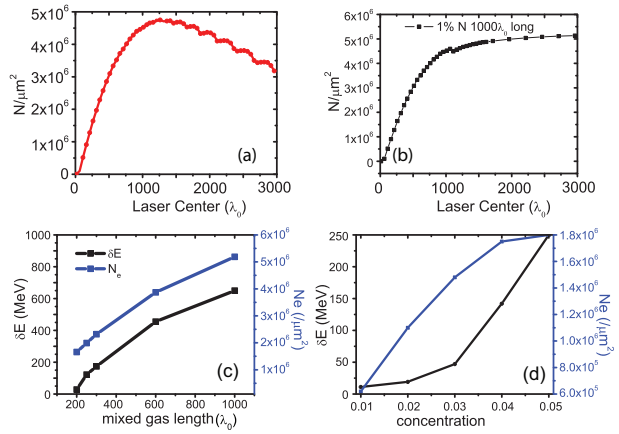

Figure 1: (a) Trapped electron number vs the length of the mixed gas traversed by laser pulse. (b) Trapped number evolution vs the laser propagation distance. Here the mixed gas length is fixed to be $1000\lambda_0$. (c) Evolution of energy spread and injected electron number along with the mixed gas length. (d) Dependence of energy spread and final electron injection number on the concentration of Nitrogen. Here the mixed gas length is $200\lambda_0$.

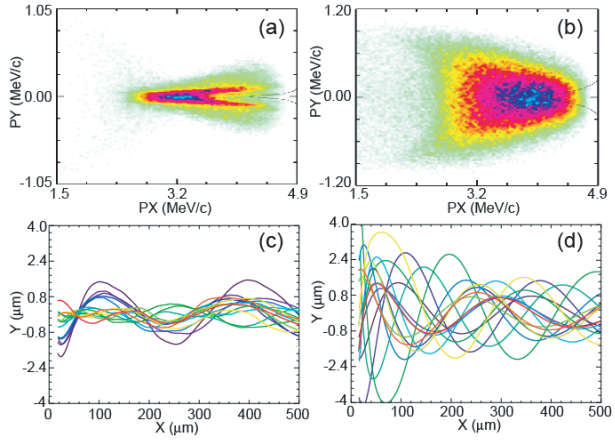

Figure 2: Transverse spatial structures of the accelerated electron beam when a S-polarized laser pulse (a) or a P-polarized laser pulse (b) is used. The acceleration length here is $94\lambda_0$. Typical trajectories of the injected electrons in the simulations corresponding to the S-polarized laser pulse (c) and the P-polarized laser pulse (d) cases, respectively.

fixed our laser intensity to be $a = 2.0$ and Full Width at Half Maximum (FWHM) to be $L_{\rm FWHM} = 14.89\,T_0$ with $T_0 = 2.67$ fs the laser period. To study the mixed gas length effect on the final beam quality we also fixed the Nitrogen concentration to be 1%. Figure 1 (a) shows the trapped electron number evolution with mixed gas length. The trapped electron number here is calculated by the criterion of Eq. 1. As we see, when the mixed gas is short, the trapped electron number linearly increases with length. However, number trapped saturates later and then decreases if the mixed gas length becomes longer. The reason is that the newly injected electrons make the beam loading effect stronger, and some of the trapped particles are lost due to this effect. If we fix the mixed gas length at the optimum length ($1000\ \lambda_0$ here) we keep the injection number at the maximum as Fig. 1 (b) shows. Fig. 1 (c) shows the simulation results of the mixed gas length effects on the beam quality. As we see, for the trapped number, the results are the same as those we get from Eq. 1. Within the region where the trapped number linearly increases with the mixed gas length, the energy spread is also almost linearly increasing. To get a high quality beam one should hence use as short a mixed gas as possible. Figure 1 (d) shows the concentration effect on the beam quality. In these simulations we fixed the mixed gas length to be $200\ \lambda_0$ but changed the Nitrogen concentration. As we see the injection number also shows the linear scaling at lower concentration and then saturates. The energy spread at first weakly depends on the concentration then increases linearly with it. This gives us some hint on the parameter selection, as one can use a relatively high concentration and short mixed gas to get the same charge and lower energy spread beam.

Multi Dimensional Effects

To study multi dimensional effects on the beam structure and reduce simulation time we conducted two dimensional simulations with different laser polarization directions. The laser pulse parameters are: $a = 2.0, L_{\rm FWHM} = 14.89\ T_0$, focus at $75\ \lambda_0$ from the simulation box boundary, the spot size is $W_{\rm FWHM} = 17.66\ \lambda_0$, and the uniform plasma density is $n_e = 0.001\ n_c$, the mixed gas length is $20\ \lambda_0$. In the first simulation the laser polarization is out of the simulation plane (S-polarization) and in the second the polarization is parallel to the simulation plane (P-Polarization). Phase-space electron beam structures of these two cases at an early acceleration time are shown in Fig. 2 (a) and (b). As we see, in the S-polarization case the electron beam shows a filament structure (or a hollow structure). In the simulation we found when the acceleration distance is small these filaments appear and merge periodically. Finally, these structures disappear when the electrons' energy is higher. We show some typical electron trajectories in Fig. 2(c) and (d) corresponding to the two cases, respectively. As we see, in the S-polarization case electrons show regular betatron oscillation and they are almost in phase at the earlier time. The period of the oscillation is the betatron wavelength $2\pi c/\omega_\beta = \sqrt{2\gamma}\lambda_p$, where γ is the relativistic factor of the electron beam and λ_p is the plasma wavelength. Over long acceleration length, the difference of the betatron phase increases which makes the betatron trajectories mix, so the filament structures disappear. On the contrary, in the P-polarization case the electrons' trajectories are initially not in phase due to the effect of the laser electric field in the same plane. Correspondingly the beam shows a normal transverse profile and its size gradually reduces due to the energy increase.

BETATRON RADIATION

When the electrons make betatron oscillations in the wakefield, they emit radiation. This gives a new kind of laser plasma based radiation source [17, 18]. To calculate such radiation a parallel C++ code named Virtual Detector for Synchrotron Radiation (VDSR) is made. The radiation intensity distribution is calculated according to the following equation:

$$\frac{d^2I}{d\omega d\Omega} = \frac{e^2\omega^2}{4\pi^2 c}\sum_j \left| \int_{-\infty}^{\infty} \vec{n}\times(\vec{n}\times\vec{\beta}_j)e^{i\omega[t-\vec{n}\cdot\vec{r}(t)/c]}dt \right|^2, \quad (2)$$

where $\vec{n}$ is the unit vector pointing to the detector pixel, $\vec{\beta}_j$ and $\vec{r}_j$ are the normalized velocity and spatial coordinates of the jth electron. VDSR reads the electrons' trajectories from the PIC simulation and then calculates every electron's radiation according to their trajectories and sums them incoherently [19].

Radiation has been modeled from a colliding pulse injection simulation using the VORPAL code [20, 21]. The driving laser parameters are the same as our ionization injection case, however the plasma is composed of preionized electrons with the density of $0.001\ n_c$. The injection is caused by a colliding pulse whose intensity is $a_1 = 0.3$ and duration is $L_{\rm FWHM} = 3.75\ T_0 \simeq 10$ fs. Figure 3 (a,b) shows the radiation distribution of the traced electrons. 1000 particles are used to represent the 1 pC electron beam. The statistical information of these particles are shown in Fig. 3 (c) and (d), in which the spread of the transverse position and longitudinal momenta are shown. The radiation is calculated after a total acceleration length of about 1.12 mm. The electron beam's center energy there is about 100MeV and the transverse radius size is about $0.75\lambda_0 = 0.6\,\mu m$. If we think of the wakefield as a hollow bubble structure, the betatron strength parameter is $a_\beta = \gamma r k_\beta = \pi\sqrt{2\gamma}r/\lambda_p \simeq 1.0$, where the average value of $<\gamma>= 100$ has been used. According to betatron radiation theory the peak radiation frequency on axis should be at $\hbar\omega_c = 2\gamma^2\hbar\omega_\beta/(1+\gamma^2\theta^2+a_\beta^2/2)$ [17]. If we use $<\gamma>= 100$ and $\hbar\omega_\beta = \hbar\omega_p/\sqrt{2<\gamma>} \simeq 0.00347$ eV, the radiation peak is at $\hbar\omega_c \simeq 45eV$ when $\theta = 0^o$. As we can see this value is close to the on axis peak photon energy in our simulation [See Fig. 3 (a) at $\theta = 0^o$]. The angularly integrated spectrum shows the radiation peak is at the photon energy of about 90 eV. This means the higher energy radiation is not exactly on axis. However most of the radiation is still within $10\text{mrad} \sim 1/<\gamma>$.

SUMMARY

In summary, ionization injection and betatron radiation were studied by multi dimensional PIC simulations. Mixed gas length and concentration effects on the ionized injected beam quality were shown. To get a high quality beam, using high concentration and short mixed gas is better than using low concentration and long mixed gas. In a low energy beam, electron filaments have been observed in the plane perpendicular to the laser polarization. Electron beam betatron radiation was also calculated by a post processing code, and the calculated results fit the betatron radiation theory well.

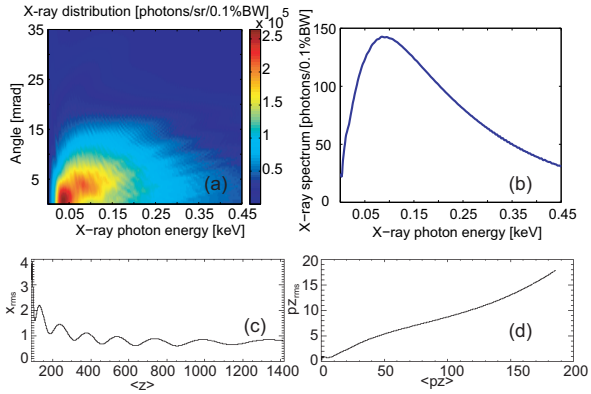

Figure 3: (a) Radiation angular and energy distribution. (b) Angularly integrated radiation spectrum distribution. Evolution of the spread of the transverse position (c) and the spread of the longitudinal momenta (d) of the traced electrons.

REFERENCES

[1] E. Esarey *et al.*, Rev. Mod. Phys. 81 (2009) 1229.
[2] W. P. Leemans *et al.*, Nature Phys. 2 (2006) 696.
[3] Nasa A. Hafz, *et al.* Nature Photonics 2 (2008) 571.
[4] S.P.D. Mangles *et al.* Nature 431 (2004) 535.
[5] C.G.R. Geddes *et al.* Nature 431 (2004) 538.
[6] J. Faure *et al.* Nature (2004) 541.
[7] E. Esarey *et al.* Phys. Rev. Lett. 79 (1997) 2682.
[8] J. Faure *et al.*, Nature 444 (2006) 737.
[9] H. Suk *et al.*, Phys. Rev. Lett. 86 (2001) 1011.
[10] C. G. R. Geddes *et al.*, Phys. Rev. Lett. 100 (2008) 215004.
[11] A. Pak *et al.*, Phys. Rev. Lett. 104 (2010) 025003.
[12] C. McGuffey *et al.*, Phys. Rev. Lett. 104 (2010) 025004.
[13] C. E. Clayton *et al.*, Phys. Rev. Lett. 105 (2010) 105003.
[14] M. Chen *et al.*, "Electron Injection in Laser Plasma Accelerators by High-Order Field Ionization," AAC'10, Annapolis, June 2010, p. 268.
[15] M. Chen *et al.*, J. Appl. Phys. 99 (2006) 056109.
[16] A. Pukhov, J. Plasma Phys. 61, (1999) 425.
[17] E. Esarey *et al.*, Phys. Rev. E 65 (2002) 056506.
[18] S. Kneip *et al.*, Nature Phys. 6 (2010) 980.
[19] A.G.R. Thomas, Phys. Rev. Spec. Topics - Acce. Beams 13 (2010) 020802.
[20] C. Nieter *et al.*, J. Compt. Phys. 196 (2004) 448.
[21] E. Cormier-Michel *et al.*, "Predictive Design of Colliding Pulse Injected Laser Wakefield Experiments", in this Proceedings.